Supplementary Material

Supplementary Methods

Supplementary Results

Supplementary Methods

For the Hotel Study sample, all scans were acquired using 3T Philips Achieva (software version 2.6.3.5) using an eight-channel SENSE head coil. High resolution 3D T1-weighted FFE sagittal images were acquired with TE = 3.7 ms, TR = 8.1 ms, flip angle 8°, FOV = 256mm × 256mm, acquisition matrix = 256 × 250, reconstruction matrix = 256 × 256, voxel spacing = 1.0 mm × 1.0 mm × 1.0 mm, 190 contiguous slices, slice thickness = 1 mm, gap = 0, SENSE = 1, scan duration = 7:23 min. Diffusion-weighted images were acquired during the same session with 70 contiguous transverse slices in 32 directions, acquisition matrix = 100 × 99, reconstruction matrix = 112 × 112, acquisition voxel = 2.24 × 2.24 × 2.0 mm, reconstructed voxel = 2.0 × 2.0 × 2.0 mm, slice thickness = 2.2 mm, TE = 60 ms, TR = 6451 ms, FOV = 224 mm × 224 mm, flip angle = 90°, SENSE = 2.1, maximum number of gradient orientations = 33, b = 700 s/mm^2, total scan duration = 3:46 min.

For the CamCAN sample, all scans were acquired on a 3T Siemens TIM Trio scanner with a 32-channel head coil. T1-weighted scans were acquired using an MPRAGE sequence, with TR = 2250ms, TE = 2.99ms, flip angle = 9°, FOV = 256 × 240 × 192mm, voxel size = 1 × 1 × 1mm, and GRAPPA 2.[1] Diffusion-weighted scans were acquired with a twice-refocused SE sequence at three b-values (b = 1000, 30 directions, 66 axial slices; b = 2000, 30 directions, 66 axial slices, and b = 0, 66 axial slices, 3 images), with TR = 9100ms, TE = 104ms, FOV = 192 × 192mm, voxel size = 2 × 2 × 2mm.

T1-weighted data from both samples was processed using FreeSurfer version 6.0 (https://surfer.nmr.mgh.harvard.edu)[2] and involved removal of non-brain tissue using a hybrid watershed/surface deformation procedure,[3] automated Talairach transformation and segmentation of the subcortical white matter and deep gray matter structures,[4,5] intensity normalization,[6] tessellation of the gray-white matter boundary, automated topology correction,[7,8] and surface deformation following intensity gradients to optimally place gray-white and gray-cerebrospinal fluid boundaries.[9–11] T1-weighted data for Hotel Study participants was evaluated by a trained research assistant and edited where necessary due to the higher pathology than the general population. T1-weighted data in the CamCAN sample was quality controlled using the ENIGMA Consortium quality control protocol (https://enigma.usc.edu/).

Diffusion tensor imaging scans for both study samples were processed using FSL (https://fsl.fmrib.ox.ac.uk; version 6.0 for CamCAN scans and version 5.0.11 for Hotel Study scans),[12] which involved brain extraction,[13] eddy current correction,[14] and tensor fitting. Additionally, for the Hotel Study scans, *eddy_cuda8.0* was used to detect and correct slices that were corrupted by motion-induced signal dropout including slice-to-volume registration. Non-diffusion volume and intensity inversed T1 volumes were used to estimate susceptibility distortion by using ANT's SyN algorithm,[15] and then mapped to T1 space and resliced as 2mm × 2mm × 2mm isotropically. All DTI volumes were then processed in FSL with tract-based spatial statistics,[16] which involved aligning individual-participant FA data into a common space using nonlinear registration, creating a mean FA image, thinning the mean FA image it into a white matter skeleton, and projecting each participants' aligned data onto the white matter skeleton.[16] Quality control was performed by a trained research assistant on the raw data, after eddy current correction, and after tensor fitting.

There was a relatively small amount of missing data for our analyses of factors associated with tissue-to-intracranial volume ratio and mean whole-brain fractional anisotropy in the precariously housed sample. HIV status was missing for 7.69%, stroke for 4.5%, traumatic brain injury history for 1.92%, IV drug use for 0.64%, and heroin dependence for 0.32%. To retain all participants in the analyses we used multiple imputation implemented through the *mice* package in R.[17,18] We used all variables included in the analyses (age, sex, tissue-to-intracranial volume ratio, mean whole-brain fractional anisotropy, mental illness diagnoses, substance dependence diagnoses, IV drug use, HIV status, and traumatic brain injury history) to impute 10 new datasets. Each regression model was fit to each imputed dataset and the results were pooled to yield the final estimates. There were no differences in the direction or statistical significance of the results between the results based on the imputed data and identical models fit on the observed data, therefore the imputed results are reported in-text and in the supplement.

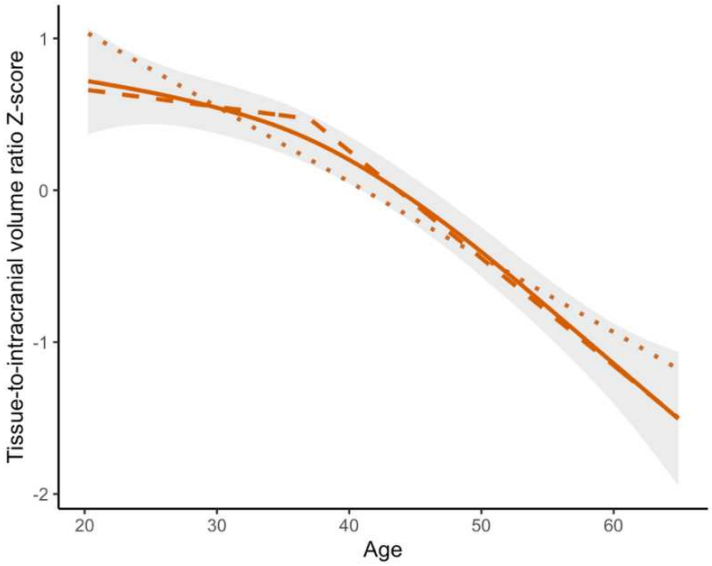

Supplementary Figure 1. Predicted values of tissue-to-intracranial volume ratio as a function of age in the Hotel Study as estimated by three different methods. Linear regression (dotted line; adjusted $R^2 = 0.265$), piecewise linear regression (dashed line; adjusted $R^2 = 0.283$), and general additive model (solid line with 95% confidence interval in shaded region; adjusted $R^2 = 0.282$).

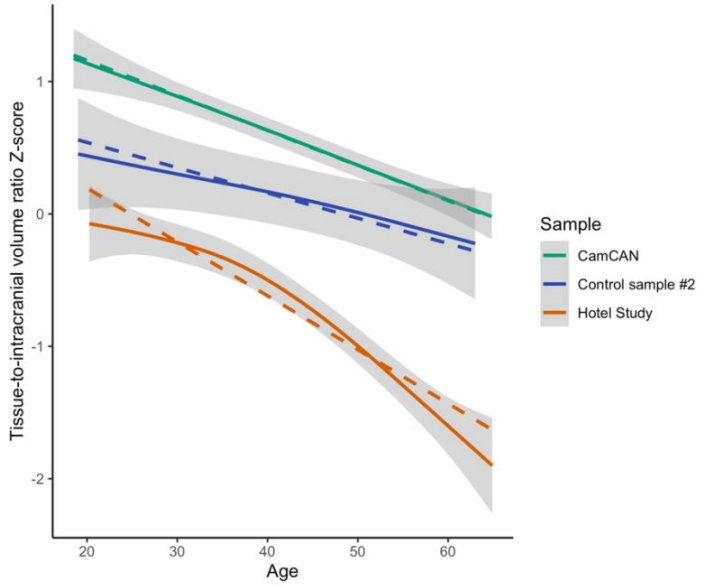

Supplementary Figure 2. Predicted values of tissue-to-intracranial volume ratio as a function of age in two healthy control samples and the Hotel Study. Linear fits (dashed) and general additive models (solid, with shaded 95% CI) are shown for the CamCAN sample (green), Hotel Study sample (orange), and an additional healthy control sample acquired on the same scanner, with the same acquisition parameters, as the Hotel Study sample (blue). A multiple linear regression model indicates that the slope of

the CamCAN sample relative to the additional healthy control sample is not significantly different (b = 0.0074, p = 0.46), while the slope of the Hotel Study relative to the additional healthy control sample is significantly different (b = 0.014, p = 0.0023). Additionally, the shape of the relationship, as visualized with a general additive model, is approximately linear for both of the healthy control samples, but it is non-linear for the Hotel Study sample.

Supplementary Results

Supplementary Table 1. Full adjusted results of whole-brain imaging outcomes.

Metric	Sample	Beta[1]	Within-group slope estimates (with break points if applicable)
Tissue-to-intracranial volume ratio[2]	General population (CamCAN)	β = -0.20, p = 0.0029	Linear: -0.39
	Precariously housed (Hotel Study)		Piecewise: -0.13 up to age 37, then -0.88
Cerebral white matter volume[3]	General population (CamCAN)	β = -0.12, p = 0.0015	Linear: 0.038
	Precariously housed (Hotel Study)		Piecewise: 0.23 up to age 39.8, then -0.33
Cortical grey matter volume[3]	General population (CamCAN)	β = -0.049, p = 0.16	Linear: -0.41
	Precariously housed (Hotel Study)		Linear: -0.36
Subcortical grey matter volume[3]	General population (CamCAN)	β = -0.060, p = 0.19	Linear: -0.35
	Precariously housed (Hotel Study)		Linear: -0.30
Fractional anisotropy (FA)[2]	General population (CamCAN)	β = -0.32, p < 0.0001	Piecewise: 0.59 up to age 30.6, then -0.47
	Precariously housed (Hotel Study)		Piecewise: -0.16 up to age 36.4, then -0.91
Mean diffusivity (MD)[2]	General population (CamCAN)	β = 0.69 p < 0.0001	Piecewise: -0.44 up to age 35.9, then 0.17
	Precariously housed (Hotel Study)		Piecewise: 0.25 up to age 43.4, then 1.34

[1]Standardized beta of the sample x age interaction term; [2]adjusted for sex; [3]adjusted for sex and intracranial volume

Supplementary Table 2. Full results of cortical thickness across regions of interest.

Region of interest	Beta[1]	p-value (unadjusted)	p-value (FDR corrected)
Banks of the superior temporal sulcus (left)	-6.50E-02	0.38	0.60
Banks of the superior temporal sulcus (right)	-5.03E-02	0.49	0.65
Caudal anterior cingulate (left)	-9.94E-02	0.18	0.47
Caudal anterior cingulate (right)	-7.83E-02	0.29	0.55
Caudal middle frontal (left)	-1.94E-01	0.0072	0.054
Caudal middle frontal (right)	8.39E-02	0.25	0.53
Cuneus (left)	2.48E-01	0.0011	0.032
Cuneus (right)	1.25E-01	0.1	0.36
Entorhinal (left)	-1.14E-01	0.14	0.40
Entorhinal (right)	-2.10E-01	0.007	0.054
Frontal pole (left)	-5.76E-02	0.46	0.64
Frontal pole (right)	-1.51E-02	0.84	0.92
Fusiform (left)	-6.54E-03	0.93	0.95
Fusiform (right)	-1.75E-02	0.82	0.92
Inferior parietal (left)	-4.83E-02	0.5	0.65
Inferior parietal (right)	-1.32E-02	0.85	0.92
Inferior temporal (left)	-1.90E-01	0.011	0.074
Inferior temporal (right)	-1.89E-01	0.012	0.074
Insula (left)	1.27E-01	0.086	0.34
Insula (right)	1.07E-01	0.14	0.40
Isthmus cingulage (left)	-6.42E-01	0.39	0.60
Isthmus cingulage (right)	-2.92E-02	0.69	0.82
Lateral occipital (left)	-5.64E-02	0.46	0.64
Lateral occipital (right)	-3.71E-02	0.63	0.77
Lateral orbitofrontal (left)	-1.09E-01	0.13	0.40
Lateral orbitofrontal (right)	-9.97E-02	0.18	0.47
Lingual (left)	4.64E-02	0.53	0.67

Lingual (right)	1.37E-01	0.067	0.28
Medial orbitofrontal (left)	-2.04E-01	0.0067	0.054
Medial orbitofrontal (right)	-1.26E-01	0.093	0.35
Middle temporal (left)	-1.49E-01	0.033	0.16
Middle temporal (right)	-2.16E-01	0.002	0.034
Paracentral (left)	7.12E-02	0.34	0.58
Paracentral (right)	8.99E-02	0.22	0.53
Parahippocampal (left)	-2.33E-02	0.76	0.89
Parahippocampal (right)	4.57E-03	0.95	0.95
Pars opercularis (left)	-6.40E-02	0.35	0.58
Pars opercularis (right)	1.60E-02	0.82	0.92
Pars orbitalis (left)	-2.45E-01	0.001	0.032
Pars orbitalis (right)	-1.66E-01	0.025	0.13
Pars triangularis (left)	-1.61E-01	0.019	0.11
Pars triangularis (right)	-8.26E-02	0.23	0.53
Pericalcarine (left)	7.41E-02	0.33	0.58
Pericalcarine (right)	-1.15E-01	0.14	0.40
Postcentral (left)	7.92E-01	0.28	0.55
Postcentral (right)	7.71E-02	0.3	0.55
Posterior cingulate (left)	-4.49E-02	0.53	0.67
Posterior cingulate (right)	-8.63E-02	0.23	0.53
Precentral (left)	-4.91E-03	0.95	0.95
Precentral (right)	-1.41E-02	0.84	0.92
Precuneus (left)	6.62E-02	0.35	0.58
Precuneus (right)	6.30E-02	0.38	0.60
Rostral anterior cingulate (left)	-6.01E-02	0.4	0.60
Rostral anterior cingulate (right)	-6.07E-02	0.42	0.62
Rostral middle frontal (left)	-7.64E-02	0.3	0.55
Rostral middle frontal (right)	-2.04E-01	0.0052	0.054
Superior frontal (left)	8.16E-03	0.9	0.94
Superior frontal (right)	-1.02E-01	0.14	0.40
Superior parietal (left)	1.10E-02	0.88	0.94
Superior parietal (right)	8.43E-02	0.25	0.53
Superior temporal (left)	-4.93E-02	0.48	0.65
Superior temporal (right)	-5.43E-02	0.44	0.64
Supramarginal (left)	8.03E-02	0.25	0.53
Supramarginal (right)	1.30E-01	0.06	0.27
Temporal pole (left)	-2.34E-01	0.0027	0.037
Temporal pole (right)	-2.49E-01	0.0014	0.032
Transverse temporal (left)	4.02E-02	0.59	0.73
Transverse temporal (right)	8.51E-02	0.26	0.54
[1]Standardized beta of the sample × age interaction term			

Supplementary Table 3. Full results of subcortical volume across regions of interest.

Region of interest	Beta[1]	p-value (unadjusted)	p-value (FDR corrected)
3rd ventricle	3.17E-01	< 0.0001	< 0.0001
4th ventricle	8.21E-02	0.26	0.35
Amygdala (left)	-8.17E-03	0.89	0.89
Amygdala (right)	-9.76E-02	0.1	0.18
Brainstem	-1.66E-02	0.77	0.80
Caudate (left)	1.45E-01	0.024	0.084
Caudate (right)	1.04E-01	0.1	0.18
Corpus callosum (anterior)	-1.75E-01	0.013	0.050
Corpus callosum (central)	-2.71E-01	0.00018	0.0012
Corpus callosum (mid-anterior)	-3.19E-01	< 0.0001	0.00017
Corpus callosum (mid-posterior)	-1.50E-01	0.041	0.11
Corpus callosum (posterior)	-1.83E-01	0.012	0.050
Hippocampus (left)	-6.43E-02	0.32	0.39
Hippocampus (right)	-8.63E-02	0.18	0.26
Lateral ventricle (left)	2.40E-01	0.00028	0.0016
Lateral ventricle (right)	2.70E-01	< 0.0001	0.00051
Pallidum (left)	-1.21E-01	0.043	0.11
Pallidum (right)	-1.15E-01	0.053	0.11
Putamen (left)	-1.21E-01	0.046	0.11
Putamen (right)	-1.04E-01	0.079	0.16
Thalamus (left)	-7.33E-02	0.17	0.26

Thalamus (right)	-2.25E-02	0.66	0.72
VentralDC (left)	-1.15E-01	0.053	0.11
VentralDC (right)	-5.75E-02	0.32	0.39
[1]Standardized beta of the sample × age interaction term			

Supplementary Table 4. Full results of white matter diffusivity across regions of interest.

	Fractional anisotropy (FA)			Mean diffusivity (MD)		
Region of interest	**Beta[1]**	**p-value**	**p-value (FDR corrected)**	**Beta[1]**	**p-value**	**p-value (FDR corrected)**
Anterior thalamic radiation (left)	-3.50E-01	< 0.0001	< 0.0001	6.10E-01	< 0.0001	< 0.0001
Anterior thalamic radiation (right)	-2.90E-01	< 0.0001	0.00015	5.20E-01	< 0.0001	< 0.0001
Cingulate gyrus (left)	-4.60E-01	< 0.0001	< 0.0001	1.90E-01	0.01	0.015
Cingulate gyrus (right)	-3.40E-01	< 0.0001	< 0.0001	1.50E-02	0.85	0.89
Hippocampus (left)	1.40E-01	0.075	0.083	-1.40E-01	0.075	0.093
Hippocampus (right)	2.30E-01	0.0025	0.0036	-2.10E-01	0.0067	0.012
Corticospinal tract (left)	-1.60E-01	0.028	0.034	4.90E-01	< 0.0001	< 0.0001
Corticospinal tract (right)	7.90E-02	0.3	0.30	-4.30E-02	0.58	0.64
Forceps major	-4.80E-01	< 0.0001	< 0.0001	3.30E-01	< 0.0001	< 0.0001
Forceps minor	-3.70E-01	< 0.0001	< 0.0001	4.50E-01	< 0.0001	< 0.0001
Inferior fronto-occipital fasciculus (left)	-3.00E-01	< 0.0001	< 0.0001	2.40E-01	0.0016	0.0031
Inferior fronto-occipital fasciculus (right)	-2.70E-01	0.00011	0.00020	1.90E-01	0.01	0.015
Inferior longitudinal fasciculus (left)	-1.90E-01	0.0088	0.012	1.60E-01	0.034	0.045
Inferior longitudinal fasciculus (right)	-2.70E-01	0.00014	0.00024	1.00E-01	0.18	0.22
Superior longitudinal fasciculus (left)	-3.00E-01	< 0.0001	< 0.0001	5.30E-01	< 0.0001	< 0.0001
Superior longitudinal fasciculus (right)	-2.40E-01	0.00072	0.0011	4.20E-01	< 0.0001	< 0.0001
Uncinate fasciculus (left)	-4.10E-01	< 0.0001	< 0.0001	6.70E-01	< 0.0001	< 0.0001
Uncinate fasciculus (right)	-3.70E-01	< 0.0001	< 0.0001	4.50E-01	< 0.0001	< 0.0001
Superior longitudinal fasciculus temporal portion (left)	-9.60E-02	0.2	0.22	2.70E-03	0.97	0.97
Superior longitudinal fasciculus temporal portion (right)	-1.50E-01	0.047	0.056	2.00E-01	0.0094	0.015
[1]Standardized beta of the sample × age interaction term						

Supplementary Table 5. Sensitivity analysis on whole-brain measures.

Metric	**Sample**	**Beta[1] with all participants included**	**Beta[1] with participants who had MRI evidence of traumatic brain injury removed**	**Beta[1] with participants who had MRI evidence of stroke removed**
	General population (CamCAN)	β = -0.20, p = 0.0029	β = -0.18, p = 0.013	β = -0.21, p = 0.0024

Tissue-to-intracranial volume ratio[1]	Precariously housed (Hotel Study)			
Cerebral white matter volume[2]	General population (CamCAN) Precariously housed (Hotel Study)	β = -0.12, p = 0.0015	β = -0.10, p = 0.010	β = -0.12, p = 0.0012
Cortical grey matter volume[2]	General population (CamCAN) Precariously housed (Hotel Study)	β = -0.049, p = 0.16	β = -0.044, p = 0.22	β = -0.048, p = 0.17
Subcortical grey matter volume[2]	General population (CamCAN) Precariously housed (Hotel Study)	β = -0.060, p = 0.19	β = -0.045, p = 0.34	β = -0.068, p = 0.14
Fractional anisotropy (FA)[1]	General population (CamCAN) Precariously housed (Hotel Study)	β = -0.32, p < 0.0001	β = -0.32, p < 0.0001	β = -0.32, p < 0.0001
Mean diffusivity (MD)[1]	General population (CamCAN) Precariously housed (Hotel Study)	β = 0.69 p < 0.0001	β = 0.68, p < 0.0001	β = 0.69, p < 0.0001
[1]Standardized beta of the sample x age interaction term; [2]adjusted for sex; [3]adjusted for sex and intracranial volume				

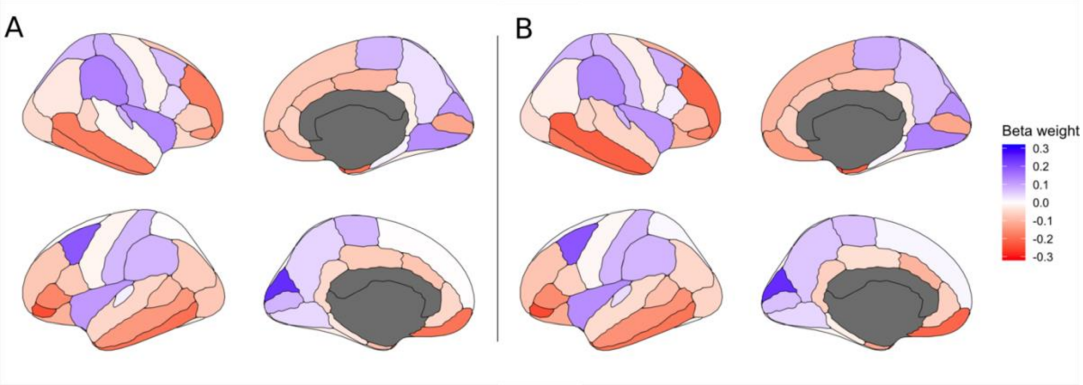

Supplementary Figure 3. Cortical regions of interest results with participants who had MRI evidence of traumatic brain injury removed (A) and participants who had MRI evidence of stroke removed (B).

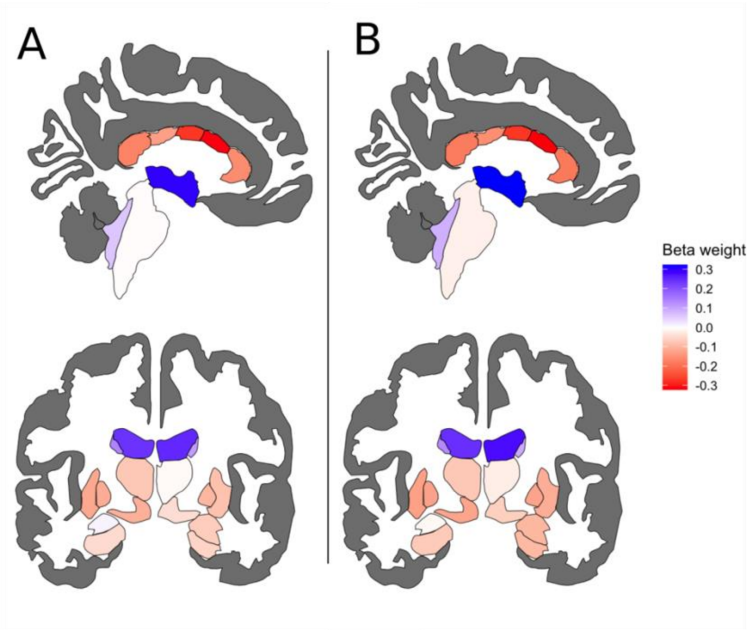

Supplementary Figure 4. Subcortical regions of interest results with participants who had MRI evidence of traumatic brain injury removed (A) and participants who had MRI evidence of stroke removed (B).

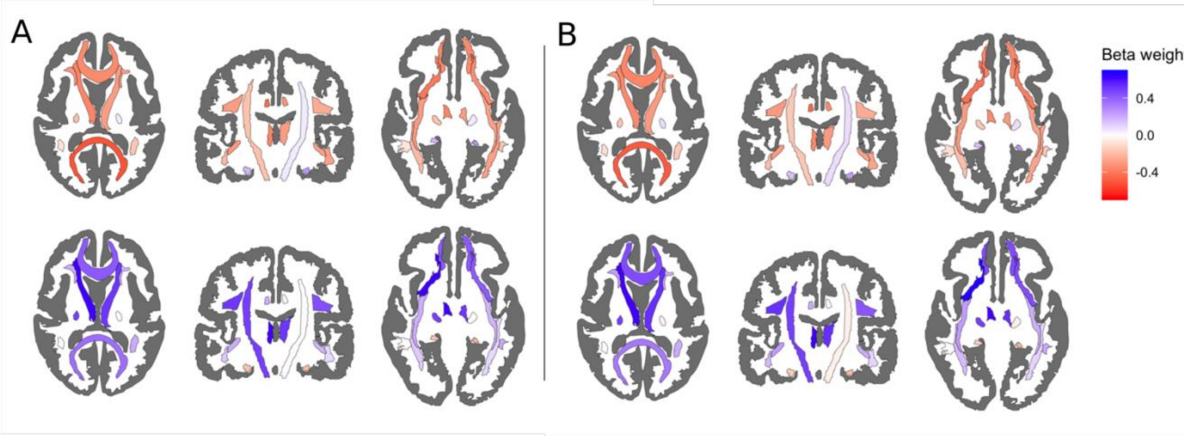

Supplementary Figure 5. White matter tract regions of interest results with participants who had MRI evidence of traumatic brain injury removed (A) and participants who had MRI evidence of stroke removed (B).

Supplementary Table 6. Full results of factors associated with tissue-to-intracranial volume ratio in the precariously housed sample.

Tissue-to-intracranial volume ratio	Block 1: Basic demographics			Block 2: Mental health diagnoses			Block 3: Substance use			Block 4: HIV, traumatic brain injury, and stroke		
	Beta	**95% CI**	***p*-value**	**Beta**	**95% CI**	***p*-value**	**Beta**	**95% CI**	***p*-value**	**Beta**	**95% CI**	***p*-value**
Age	0.56	-0.15, 1.27	0.12	0.55	-0.19, 1.28	0.14	0.49	-0.30, 1.27	0.22	0.46	-0.32, 1.23	0.25
Age^2	-1.12	-1.83, -0.40	0.0022	-1.13	-1.86, -0.40	0.0027	-1.08	-1.85, -0.31	0.0062	-1.01	-1.77, -0.25	0.0098
Sex												
Female	—	—		—	—		—	—		—	—	
Male	-0.51	-0.75, -0.27	< 0.0001	-0.45	-0.70, -0.20	0.00047	-0.43	-0.70, -0.17	0.0013	-0.47	-0.73, -0.21	0.00049
Schizophrenia				-0.29	-0.65, 0.06	0.11	-0.31	-0.67, 0.06	-0.10	-0.28	-0.63, 0.08	0.13
Schizoaffective				-0.05	-0.39, 0.28	0.76	-0.05	-0.39, 0.29	0.78	-0.04	-0.38, 0.30	0.81
Bipolar I or Bipolar NOS				0.10	-0.28, 0.48	0.60	0.11	-0.27, 0.50	0.56	0.13	-0.25, 0.51	0.49
Bipolar II				0.12	-0.37, 0.62	0.63	0.13	-0.38, 0.63	0.62	0.10	-0.40, 0.60	0.69
Major depressive disorder or depression NOS				0.16	-0.14, 0.46	0.31	0.16	-0.15, 0.46	0.32	0.16	-0.15, 0.47	0.3
Psychotic disorder NOS				-0.21	-0.55, 0.12	0.22	-0.22	-0.56, 0.13	0.21	-0.17	-0.51, 0.16	0.31
Alcohol							-0.01	-0.27, 0.25	0.94	-0.01	-0.27, 0.24	0.92
Stimulant							0.06	-0.22, 0.35	0.66	0.04	-0.24, 0.32	0.79
Heroin							-0.01	-0.24, 0.22	0.95	0.01	-0.22, 0.24	0.94
Cannabis							-0.10	-0.33, 0.13	0.38	-0.12	-0.35, 0.10	0.29
IV drug use							-0.07	-0.35, 0.22	0.65	-0.03	-0.30, 0.25	0.85
HIV positivity										-0.16	-0.47, 0.16	0.32
Traumatic brain injury										-0.35	-0.56, -0.13	0.0017
Stroke										-0.42	-0.85, 0.01	0.056

*NOS = not otherwise specified

Supplementary Table 7. Full results of factors associated with whole-brain fractional anisotropy (FA) in the precariously housed sample.

Average whole-brain fractional anisotropy (FA)	Block 1: Basic demographics			Block 2: Mental health diagnoses			Block 3: Substance use			Block 4: HIV, traumatic brain injury, and stroke		
	Beta	**95% CI**	***p*-value**	**Beta**	**95% CI**	***p*-value**	**Beta**	**95% CI**	***p*-value**	**Beta**	**95% CI**	***p*-value**
Age	0.48	-0.30, 1.27	0.23	0.46	-0.35, 1.27	0.27	0.31	-0.54, 1.16	0.48	0.27	-0.59, 1.13	0.54
Age^2	-1.11	-1.90, -0.33	0.0056	-1.11	-1.92, -0.30	0.0075	-0.96	-1.80, -0.13	0.024	-0.89	-1.73, -0.04	0.039
Sex												
Female	—	—		—	—		—	—		—	—	
Male	0.20	-0.07, 0.47	0.15	0.23	-0.05, 0.51	0.11	0.16	-0.12, 0.45	0.26	0.12	-0.17, 0.41	0.41
Schizophrenia				-0.24	-0.63, 0.16	0.24	-0.30	-0.70, 0.09	0.13	-0.28	-0.67, 0.11	0.16
Schizoaffective				0.16	-0.21, 0.53	0.4	0.13	-0.24, 0.5	0.49	0.15	-0.22, 0.52	0.43
Bipolar I or Bipolar NOS				-0.20	-0.62, 0.23	0.36	-0.17	-0.58, 0.25	0.43	-0.18	-0.60, 0.23	0.39
Bipolar II				0.06	-0.49, 0.61	0.83	0.10	-0.45, 0.65	0.72	0.04	-0.51, 0.59	0.89
Major depressive disorder or depression NOS				-0.07	-0.40, 0.26	0.67	0.02	-0.31, 0.36	0.90	0.05	-0.28, 0.39	0.76
Psychotic disorder NOS				-0.05	-0.43, 0.32	0.78	-0.01	-0.38, 0.36	0.95	0.03	-0.35, 0.40	0.89
Alcohol							-0.22	-0.50, 0.07	0.13	-0.22	-0.51, 0.06	0.12
Stimulant							0.33	0.02, 0.64	0.035	0.34	0.03, 0.65	0.034
Heroin							-0.28	-0.53, -0.03	0.030	-0.28	-0.53, -0.03	0.031
Cannabis							0.18	-0.06, 0.43	0.15	0.18	-0.07, 0.42	0.16
IV drug use							-0.02	-0.32, 0.29	0.92	0.00	-0.31, 0.30	0.99
HIV positivity										-0.23	-0.58, 0.11	0.19
Traumatic brain injury										-0.09	-0.33, 0.15	0.46
Stroke										-0.47	-0.95, 0.01	0.054

*NOS = not otherwise specified

Supplementary References

1. Taylor, J. R. *et al.* The Cambridge Centre for Ageing and Neuroscience (Cam-CAN) data repository: Structural and functional MRI, MEG, and cognitive data from a cross-sectional adult lifespan sample. *NeuroImage* **144**, 262–269 (2017).
2. Fischl, B. FreeSurfer. *NeuroImage* **62**, 774–781 (2012).
3. Ségonne, F. *et al.* A hybrid approach to the skull stripping problem in MRI. *NeuroImage* **22**, 1060–1075 (2004).
4. Fischl, B. *et al.* Whole brain segmentation: automated labeling of neuroanatomical structures in the human brain. *Neuron* **33**, 341–355 (2002).
5. Fischl, B. *et al.* Sequence-independent segmentation of magnetic resonance images. *NeuroImage* **23 Suppl 1**, S69-84 (2004).
6. Sled, J. G., Zijdenbos, A. P. & Evans, A. C. A nonparametric method for automatic correction of intensity nonuniformity in MRI data. *IEEE Trans. Med. Imaging* **17**, 87–97 (1998).
7. Fischl, B., Liu, A. & Dale, A. M. Automated manifold surgery: constructing geometrically accurate and topologically correct models of the human cerebral cortex. *IEEE Trans. Med. Imaging* **20**, 70–80 (2001).
8. Ségonne, F., Pacheco, J. & Fischl, B. Geometrically accurate topology-correction of cortical surfaces using nonseparating loops. *IEEE Trans. Med. Imaging* **26**, 518–529 (2007).
9. Dale, A. M., Fischl, B. & Sereno, M. I. Cortical Surface-Based Analysis: I. Segmentation and Surface Reconstruction. *NeuroImage* **9**, 179–194 (1999).
10. Dale, A. M. & Sereno, M. I. Improved Localizadon of Cortical Activity by Combining EEG and MEG with MRI Cortical Surface Reconstruction: A Linear Approach. *J. Cogn. Neurosci.* **5**, 162–176 (1993).
11. Fischl, B. & Dale, A. M. Measuring the thickness of the human cerebral cortex from magnetic resonance images. *Proc. Natl. Acad. Sci.* **97**, 11050–11055 (2000).

12. Smith, S. M. *et al.* Advances in functional and structural MR image analysis and implementation as FSL. *NeuroImage* **23**, S208–S219 (2004).

13. Smith, S. M. Fast robust automated brain extraction. *Hum. Brain Mapp.* **17**, 143–155 (2002).

14. Andersson, J. L. R. & Sotiropoulos, S. N. An integrated approach to correction for off-resonance effects and subject movement in diffusion MR imaging. *NeuroImage* **125**, (2015).

15. Avants, B. B., Epstein, C. L., Grossman, M. & Gee, J. C. Symmetric diffeomorphic image registration with cross-correlation: evaluating automated labeling of elderly and neurodegenerative brain. *Med. Image Anal.* **12**, 26–41 (2008).

16. Smith, S. M. *et al.* Tract-based spatial statistics: Voxelwise analysis of multi-subject diffusion data. *NeuroImage* **31**, 1487–1505 (2006).

17. van Buuren, S. mice: Multivariate imputation by chained equations. R package version 3.13.0. (2021).

18. van Buuren, S. & Groothuis-Oudshoorn, k. mice: Multivariate Imputation by Chained Equations in R. **45**, 1–67 (2011).